Asian Journal of Chemistry; Vol. 38, No. 5 (2026), 1361-1366
ASIAN JOURNAL OF CHEMISTRY
https://doi.org/10.14233/ajchem.2026.35812

Synthesis, Spectral Analysis, *in vitro* Evaluation and Molecular Docking of 4-Chloro-1*H*-pyrrolo[2,3-*b*]pyridine-3-amines as Anticancer Agents

YADALA PRAPURNA CHANDRA[1], SHAIK ASMA PARVEEN[1,*], BEEBI JAN KALLURI[2], Y. SRIBHARATHI[1] and GUNTAKA RAMACHANDRA REDDY[3]

[1]Ratnam Institute of Pharmacy, Pidathapolur, Nellore-524411, India
[2]Department of Pharmaceutical Analysis, Ratnam Institute of Pharmacy, Pidathapolur, Nellore-524411, India
[3]Faculty of Pharmacy, Sree Balaji Medical College Hospital, Chennai-600044, India

*Corresponding author: E-mail: asmaparveen.shk@gmail.com

Received: 10 March 2026 *Accepted*: 22 April 2026 *Published online*: 4 May 2026 AJC-22362

Azaindole-based scaffolds are recognised for their diverse pharmacological properties, including anticancer, anti-angiogenic, antioxidant, antibacterial, antifungal and anti-inflammatory activities. In present study, a novel series of 4-chloro-1*H*-pyrrolo[2,3-*b*]pyridine-3-amine derivatives was synthesised and characterised to investigate their potential as poly(ADP-ribose) polymerase-1 (PARP1) inhibitors for anticancer therapy. The synthesised derivatives were evaluated for anticancer activity against MCF-7 breast cancer cell lines using the MTT assay method. Among the tested compounds, **5b**, **5g**, **5h** and **5a** demonstrated notable cytotoxic activity against breast cancer cells. The molecular docking studies were further performed against the PARP1 target protein (PDB ID: 7KK4) to examine ligand–protein interactions and binding affinity. The computational analysis revealed that compounds **5e** and **5c** exhibited favourable binding interactions within the active site, suggesting their potential as promising PARP1 inhibitory candidates for further anticancer investigations.

Keywords: Chloroazaindole, Phenylamine derivatives, Pyrrolo-pyridine amines, PARP1 Inhibitors, Anticancer activity.

INTRODUCTION

Pyridine- and pyrrole-containing heterocycles constitute important structural motifs in medicinal chemistry because of their broad spectrum of pharmacological activities and therapeutic applications [1-4]. Pyridine derivatives, in particular, have attracted considerable attention owing to their significant antitumour and anticancer properties against various cancer cell lines including MCF-7 and HepG-2 [5-14]. Several pyridine based analogues such as picolinamide and fused pyridine derivatives, have demonstrated potent antiproliferative and VEGFR-2 inhibitory activities against colorectal adenocarcinoma (HT-29), pancreatic cancer (PANC-1), hepatoma (HepG-2) and breast cancer (MCF-7) cell lines [10-13].

Similarly, pyrrole-based heterocyclic systems are associated with diverse biological activities including antibacterial, anti-inflammatory, antiseptic, lipid-lowering, and anticancer effects [15-18]. Recent investigations have shown that pyrrolo-[2,3-*d*]pyrimidine and azaindole derivatives exhibit promising anticancer potential through inhibition of multiple molecular targets such as epidermal growth factor receptor (EGFR), Janus kinases (JAK), carbonic anhydrase and murine double minute-2 (MDM-2) proteins [19-21]. In addition, aryl urea containing heterocycles form key pharmacophoric elements in clinically important tyrosine kinase inhibitors including sorafenib and linifanib [22].

Breast cancer remains one of the most commonly diagnosed malignancies and a major cause of cancer-related mortality among women worldwide [23,24]. The MCF-7 breast cancer cell line, characterised by estrogen receptor positivity and estrogen-responsive proliferation, is extensively employed as an experimental model for evaluating anti-estrogen therapies and investigating mechanisms of drug resistance [12,23,24]. Despite advances in targeted therapeutics, the treatment of advanced breast cancer continues to face significant challenges due to tumour heterogeneity, resistance development, and inadequate immune infiltration [23,24]. Recently, the U.S. FDA approved imlunestrant, an oral selective estrogen receptor degrader (SERD), for the treatment of hormone receptor-positive (HR^+)/HER2-negative, ESR1-mutated advanced or

This is an open access journal, and articles are distributed under the terms of the Attribution 4.0 International (CC BY 4.0) License. This license lets others distribute, remix, tweak, and build upon your work, even commercially, as long as they credit the author for the original creation. You must give appropriate credit, provide a link to the license, and indicate if changes were made.

metastatic breast cancer, highlighting the continuing need for novel targeted therapeutic agents [14].

Poly(ADP-ribose) polymerase-1 (PARP1) has emerged as an important molecular target in anticancer drug discovery due to its central role in DNA damage detection and repair pathways [25,26]. The pharmacological inhibition of PARP1 results in the accumulation of unrepaired DNA lesions, ultimately leading to tumour cell death, particularly in cancers with defective DNA repair mechanisms such as breast and ovarian cancers [25,26]. Consequently, the development of novel PARP1 inhibitors based on heterocyclic scaffolds represents a promising strategy for anticancer therapy.

In view of the pharmacological significance of azaindole-based heterocycles and the therapeutic relevance of PARP1 inhibition, the present study focuses on the synthesis and characterisation of a new series of 4-chloro-1*H*-pyrrolo[2,3-*b*]-pyridine-3-amine derivatives derived from 4-chloro-7-aza-indole (**5a-g**). The synthesised compounds were evaluated for their anticancer activity against MCF-7 breast cancer cell lines using the MTT assay method. Furthermore, molecular docking studies were carried out against the PARP1 receptor protein (PDB ID: 7KK4) to investigate ligand-protein interactions and binding affinity profiles [27,28].

EXPERIMENTAL

All the required reagents and chemicals were procured from Sigma-Aldrich. Reaction progress was monitored by TLC using silica gel G precoated plates and visualised under UV light (λ = 254 nm) and iodine vapours. Melting points were deter-mined using a digital melting point apparatus. FTIR spectra were recorded using Shimadzu IR 460 spectrophotometer, while ^{1}H and ^{13}C NMR spectra were obtained using a Bruker NMR spectrometer (500 MHz) with tetramethylsilane (TMS) as internal standard.

Synthesis of 4-chloro-*N*-(2-chlorophenyl)-1*H*-pyrrolo-[2,3-*b*]pyridine-3-amine derivatives (5a-h): 4-Chloro-7-azaindole (**1**) (0.01 mol) was reacted with trichloroacetic acid and $AlCl_3$ (0.01 mol) in dichloromethane (25 mL) under reflux for 2 h. After completion of the reaction, the product was filtered, dried, and purified to afford intermediate (**2**). The intermediate was subsequently refluxed with tosyl chloride to obtain compound **3**, which on further treatment with thionyl chloride and KOH in ethanol under reflux for 45 min yielded intermediate **4**. The resulting product was recrystallised and further reacted with substituted phenylamine derivatives in the presence of KOH/ethanol to furnish the final 4-chloro-1*H*-pyrrolo[2,3-*b*]-pyridine-3-amine derivatives (**5a-h**) (**Scheme-I**). The final compounds were isolated by filtration, dried and purified through recrystallisation.

4-Chloro-*N*-(2-chlorophenyl)-1*H*-pyrrolo[2,3-*b*]pyridine-3-amine (5a): Light yellow solid, yield: 65%, m.p.: 179-181 ºC; ^{1}H NMR (500 MHz, chloroform-d_6, δ ppm): 6.86 (d, 1H), 7.27 (M, 1H), 7.43 (d, 1H), 7.59 (d, 2H), 7.75 (d, 1H), 8.46 (d, 1H), 9.25 (s, 1H), 9.28 (s, 1H); ^{13}C NMR (125 MHz, chloroform-d_6, δ ppm): 100.5, 115.5, 121.9, 122.9, 122.2, 123.4, 125.6, 127.8, 130.8, 134.2, 136.8, 143.9, 150.2. HRMS: *m/z* for $C_{13}H_9Cl_2N_3$ ($[M+H]^+$): 277.14; found 278.16.

4-Chloro-*N*-(2,4-dichlorophenyl)-1*H*-pyrrolo[2,3-*b*]-pyridine-3-amine (5b): Light yellow powder, yield: 68%, m.p.: 167-168 ºC; ^{1}H NMR (500 MHz, chloroform-d_6, δ ppm): 6.86 (d, 1H), 7.06 (m, 1H), 7.14 (d, 1H), 7.45 (d, 2H), 7.59 (d, 1H), 8.46 (d, 1H), 9.25 (s, 1H), 9.58 (s, 1H); ^{13}C NMR (125 MHz, chloroform-d_6, δ ppm): 100.4, 115.5, 119.2, 121.7, 123.4, 125.6, 126.8, 127.7, 131.8, 134.3, 143.9, 150.3. HRMS: *m/z* for $C_{13}H_8Cl_3N_3$ ($[M+H]^+$): 311.58; found 312.59.

4-Chloro-*N*-(4-chloro-3-nitrophenyl)-1*H*-pyrrolo[2,3-*b*]-pyridine-3-amine (5c): Yellow crystal, yield: 63%, m.p.: 157-158 ºC; ^{1}H NMR (500 MHz, chloroform-d_6, δ ppm): 6.86 (d, 1H), 7.06 (m, 1H), 7.14 (d, 1H), 7.45 (d, 2H), 7.59 (d, 1H), 8.46 (d, 1H), 9.25 (s, 1H), 9.58 (s, 1H); ^{13}C NMR (125 MHz, chloroform-d_6, δ ppm): 100.5, 110.6, 115.9, 117.9, 121.2, 123.4, 128.6, 130.8, 134.2, 141.8, 143.9, 1480.2, 150.5. HRMS: *m/z* for $C_{13}H_8Cl_2N_4O_2$ ($[M+H]^+$): 322.00; found 323.13.

4-Chloro-*N*-(4-fluorophenyl)-1*H*-pyrrolo[2,3-*b*]pyridine-3-amine (5d): Light brown solid, yield: 65%. m.p, 189-191 ºC; ^{1}H NMR (500 MHz, chloroform-d_6, δ ppm): 6.86 (d, 1H), 7.26 (m, 1H), 7.29 (d, 1H), 7.38 (d, 2H), 7.45 (d, 1H), 8.46 (d, 1H), 9.78 (s, 1H); ^{13}C NMR (125 MHz, chloroform-d_6, δ ppm): 100.5, 114.5, 115.9, 118.9, 121.2, 121.4, 123.6, 139.8, 143.8, 148.9, 150.2. HRMS: *m/z* $C_{13}H_9ClN_3F$ for ($[M+H]^+$): 261.05; found 261.68.

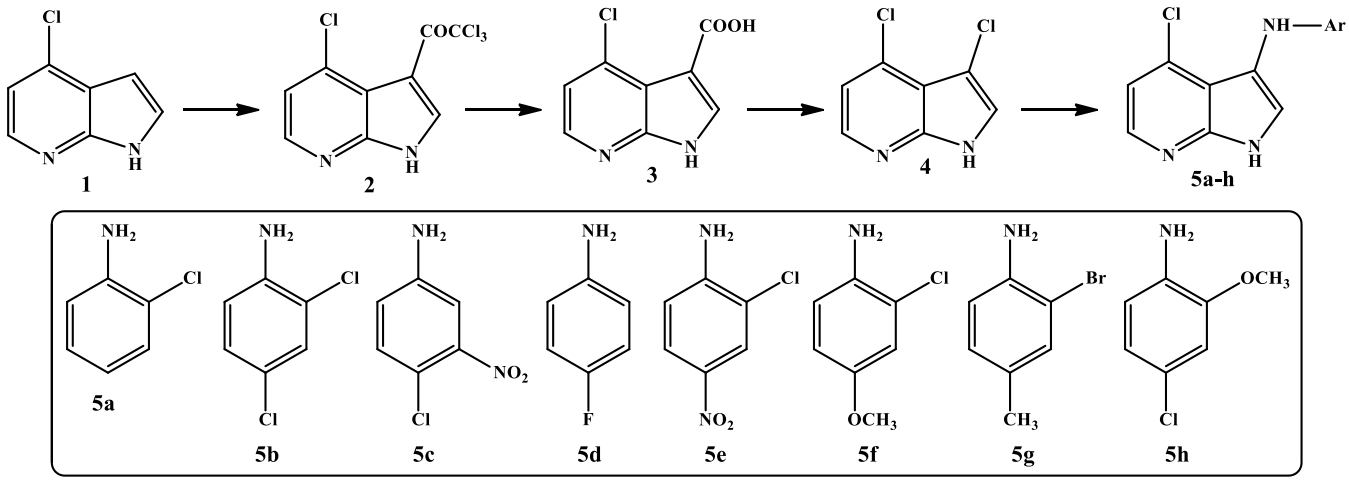

Scheme-I: Synthetic route of 4-chloro-1*H*-pyrrolo[2,3-*b*]pyridine-3-amines (**5a-h**)

4-Chloro-*N*-(2-chloro-4-nitrophenyl)-1*H*-pyrrolo[2,3-*b*]-pyridine-3-amine (5e): Brown solid powder, yield: 62%. m.p.: 198-211 ºC; ^{1}H NMR (500 MHz, chloroform-d_6, δ ppm): 6.86 (d, 1H), 7.31 (m, 1H), 7.34 (d, 1H), 7.42 (d, 2H), 7.43 (d, 1H), 7.46 (d, 1H), 8.42 (s, 1H), 9.68 (s, 1H), 9.72 (s, 1H). ^{13}C NMR (125 MHz, chloroform-d_6, δ ppm): 100.5, 115.5, 116.3, 116.9, 121.2, 123.4, 123.6, 123.8, 134.2, 141.8, 143.2, 150.2, 157.8. HRMS: *m/z* for $C_{13}H_9Cl_2N_4O_2$ ([M+H]$^+$): 322.00; found 323.13.

4-Chloro-*N*-(2-chloro-4-methoxyphenyl)-1*H*-pyrrolo-[2,3-*b*]pyridine-3-amine (5f): Light yellow solid, yield: 75%. m.p.: 212-218 ºC; ^{1}H NMR (500 MHz, chloroform-d_6, δ ppm): 6.86 (d, 1H), 7.36 (m, 1H), 7.43 (d, 1H), 7.91 (d, 2H), 8.15 (d, 1H), 8.42 (d, 1H), 9.23 (s, 1H), 9.58 (s, 1H); ^{13}C NMR (125 MHz, chloroform-d_6, δ ppm): 100.5, 115.5, 118.9, 121.9, 122.8, 123.4, 125.6, 126.8, 134.8, 139.2, 142.8, 143.9, 150.3. HRMS: *m/z* for $C_{14}H_{11}Cl_2N_3O$ ([M+H]$^+$): 307.03; found 308.16.

4-Chloro-*N*-(2-bromo-4-methylphenyl)-4-chloro-1*H*-pyrrolo[2,3-*b*]pyridine-3-amine (5g): Light brown crystal, yield: 72%. m.p.: 165-168 ºC; ^{1}H NMR (500 MHz, chloroform-d_6, δ ppm): 2.36 (d, 3H), 6.86 (d, 1H), 7.02 (m, 1H), 7.09 (d, 1H), 7.24 (d, 2H), 7.45 (d, 1H), 8.42 (d, 1H), 9.25 (s, 1H), 9.58 (s, 1H); ^{13}C NMR (125 MHz, chloroform-d_6, δ ppm): 20.7, 100.5, 115.5, 117.9, 118.9, 121.2, 123.4, 128.6, 130.8, 134.2, 134.8, 143.9, 147.3, 150.2. HRMS: *m/z* for $C_{14}H_{11}ClBrN_3$ ([M+H]$^+$): 334.98; found 336.63.

4-Chloro-*N*-(2-chloro-4-methoxyphenyl)-1*H*-pyrrolo-[2,3-*b*]pyridine-3-amine (5h): Yellow solid powder, yield: 69%. m.p.: 169-171 ºC; ^{1}H NMR (500 MHz, chloroform-d_6, δ ppm): 3.81 (d, 3H), 6.68 (d, 1H), 6.86 (m, 1H), 7.14 (d, 1H), 7.25 (d, 2H), 7.49 (d, 1H), 8.46 (d, 1H), 9.25 (s, 1H), 9.58 (s, 1H); ^{13}C NMR (125 MHz, chloroform-d_6, δ ppm): 55.8, 100.5, 113.5, 115.5, 115.9, 118.2, 121.4, 123.6, 126.5, 126.8, 134.2, 143.8, 150.9, 152.2. HRMS: *m/z* for $C_{14}H_{11}Cl_2ON_3$ ([M+H]$^+$): 307.03; found 308.16.

***In vitro* Biological activity by MTT assay method:** Human breast cancer MCF-7 cell lines were cultured in RPMI-1640 medium supplemented with 2 mM L-glutamine and 5% fetal bovine serum. The cells were seeded into 96-well microtiter plates (100 μL/well) and incubated for 24 h at 37 ºC in a humidified atmosphere containing 5% CO_2 and 95% air. After incubation, different concentrations of the test compounds were added to the respective wells containing fresh medium, followed by further incubation for 48 h under identical conditions. The assay was terminated by the addition of cold trichloroacetic acid to fix the adherent cells and the plates were incubated at 4 ºC for 1 h. The supernatant was discarded and the plates were washed repeatedly with distilled water and finally air-dried. Subsequently, 100 μL of 0.4% sulforhodamine B solution prepared in 1% acetic acid was added to each well and allowed to stain the cells for 10 min. Excess dye was removed by washing with 1% acetic acid, and the plates were dried. The protein-bound dye was then dissolved in 10 mM Trizma base and absorbance was measured at 515 nm using a microplate reader to determine cell viability and anticancer activity.

Three dose–response parameters were determined for each tested compound. The GI_{50} value, defined as the concentration required to inhibit 50% of cell growth, was calculated using the following formula:

$$\frac{Ti - Tz}{C - Tz} \times 100 = 50$$

where 50 is the drug concentration, GI_{50} was calculated.

Molecular docking: Docking studies were performed to identify novel breast cancer drugs by observing the molecular interactions of designed ligands with PARP1 receptor protein. The selection of the target protein for docking is based on several factors such as it must possess resolution less than 2.0 Å, the structure should be determined by X-ray diffraction, it consists of co-crystallised ligand and it does not have any protein breaks in the selected protein's 3D structure. PARP1 receptor protein is the recently exploring target for the identification of breast cancer drugs possessing an pyrrolopyrimidine nucleus. The crystal structure of the PARP1 target receptor protein was obtained from the protein databank PDB ID: 7KK4 having resolution of 1.96 Å. AutoDock 4.2.6 software was utilised to know the type of interactions of the designed 3D-structured pyrrolopyrimidines with the 7KK4 active site region. ChemSketch, version 2022.1.2, ACD/Labs software was used to draw the designed structures and they were converted into suitable 3D models. By applying molecular mechanics they were subjected to energy minimisations, which are required for molecular docking and for the preparation of corresponding pdb files. Docking studies were preformed to find out the possible locations for the ligand in the active site region of the receptor. Grid-based docking studies was carried out using default parameters and docking was performed by considering Olaparib as reference ligands at PARP1 active site. Discovery Studio visualizer v21.1 is used to check the 2D and 3D interactions of ligands with target [27,28].

RESULTS AND DISCUSSION

A series of novel 4-chloro-1*H*-pyrrolo[2,3-*b*]pyridine-3-amine derivatives (**5a-h**) was successfully synthesised from 4-chloro-7-azaindole through sequential chlorination, tosylation, cyclisation and nucleophilic substitution reactions with substituted phenylamines. The target compounds were obtained in good yields (62-75%) as crystalline solids with distinct melting points.

The structures of the synthesised compounds were confirmed by ^{1}H NMR, ^{13}C NMR and HRMS analyses. In the ^{1}H NMR spectra, aromatic proton signals corresponding to the pyrrolopyridine and substituted phenyl rings appeared within the δ 6.68-8.46 ppm region, while singlets observed around δ 9.2-9.7 ppm confirmed the NH proton of the azaindole framework. Substituent-specific signals such as methyl (δ ~2.36 ppm) and methoxy (δ ~3.81 ppm) resonances further supported the assigned structures. The ^{13}C NMR spectra displayed characteristic aromatic and heterocyclic carbon signals within the expected chemical shift range, confirming the fused pyrrolopyridine scaffold. HRMS spectra showed molecular ion peaks ([M+H]$^+$) consistent with the calculated molecular masses of the respective compounds, including the expected isotopic patterns for halogen-containing derivatives.

Molecular docking: Molecular docking analysis was performed to investigate the binding interactions of the synthesised 4-chloro-1*H*-pyrrolo[2,3-*b*]pyridine-3-amine derivatives (**5a-h**) with the PARP1 receptor protein (PDB ID: 7KK4). The docking results provided information regarding binding energy, hydrogen bonding interactions, bond lengths and amino acid residues involved in ligand stabilisation within the active site (Table-1). Olaparib was used as the reference ligand and exhibited a binding energy of -10.22 kcal/mol.

Among the synthesised compounds, derivatives **5e** and **5c** demonstrated the most favourable binding affinities with docking scores of -8.95 and -8.68 kcal/mol, respectively, indicating strong interaction with the PARP1 active site. Compound **5e** formed multiple stabilising interactions, including hydrogen bonding and hydrophobic contacts with key amino acid residues such as SER904, ASN767 and GLY863, which contributed to enhanced binding stability. Similarly, compound **5c** exhibited favourable interactions with important active site residues through hydrogen bonding and π- interactions, supporting effective ligand accommodation within the receptor cavity. The remaining compounds showed moderate binding affinities ranging from -7.54 to -8.34 kcal/mol, indicating acceptable interaction potential with the target protein. Halogen substituents such as chloro, bromo and nitro groups appeared to contribute significantly to receptor binding through hydrophobic and electrostatic interactions. The presence of azaindole and pyrrolopyridine nuclei further enhanced ligand orientation and stabilisation within the catalytic pocket of PARP1.

The 2D and 3D interaction diagrams (Figs. 1-3) revealed that the synthesised ligands occupied the active binding pocket in a manner comparable to the reference ligand olaparib. The interaction profiles suggest that these compounds may effectively inhibit PARP1 activity through stable ligand-protein complex formation. Thus, the docking study identified compounds **5e** and **5c** as the most promising candidates of the series for further anticancer investigation targeting PARP1.

Biological activity: All the synthesised compounds (**5a-h**) were evaluated for their anticancer activity against the human breast cancer MCF-7 cell line using the MTT assay method, with olaparib employed as the reference standard. The results presented in Table-2 demonstrated that the compounds exhibited moderate to significant cytotoxic activity, with GI_{50} values ranging from 12.11 to 135.12 μM. Among the tested derivatives, compound **5b** showed the highest anticancer activity with a GI_{50} value of 12.11 μM, indicating superior growth inhibitory potential against MCF-7 cells. Compounds **5g** and **5f** also displayed notable cytotoxic activity with GI_{50} values of 14.21 and 15.62 μM, respectively, while compounds **5a** and **5d** exhibited moderate activity with GI_{50} values of 22.14 and 26.41 μM.

The enhanced activity observed for compounds **5b**, **5g**, and **5f** may be attributed to the presence of electron-withdrawing substituents such as chloro and bromo groups, which could improve hydrophobic interactions and cellular uptake, thereby enhancing antiproliferative activity. In contrast, compounds **5c** and **5h** showed comparatively lower anticancer activity, possibly due to the presence of nitro substituents on the phenyl ring, which

TABLE-1
DETAILS OF SYNTHESISED COMPOUNDS (**5a-h**) WITH DOCKING SCORES, H-BOND INTERACTION AND AMINO ACID RESIDUES

Compound	KI	Binding scores	Amino acid residues	H-Bond distance	H-Bond interactions
5a	4.17 μM	7.34	SER904	1.9	1
5b	1.1 μM	8.13	SER904	1.88	1
5c	431.77 μM	8.68	GLY863, ARG865, SER904	1.84, 2.87, 1.80	3
5d	6.61 μM	7.07	SER904	1.87	1
5e	276.73 μM	8.95	ASN767, SER864, ARG865, GLY863	2.02, 3.02, 2.07, 2.35, 2.31	5
5f	1.68 μM	7.88	SER864, ARG865, SER904	2.56, 2.16, 2.08	3
5g	1.25 μM	8.05	NA	–	0
Std.	32.39 nM	10.22	GLY863, TYR896, SER904	2.09,3.18, 2.94, 1.86	4

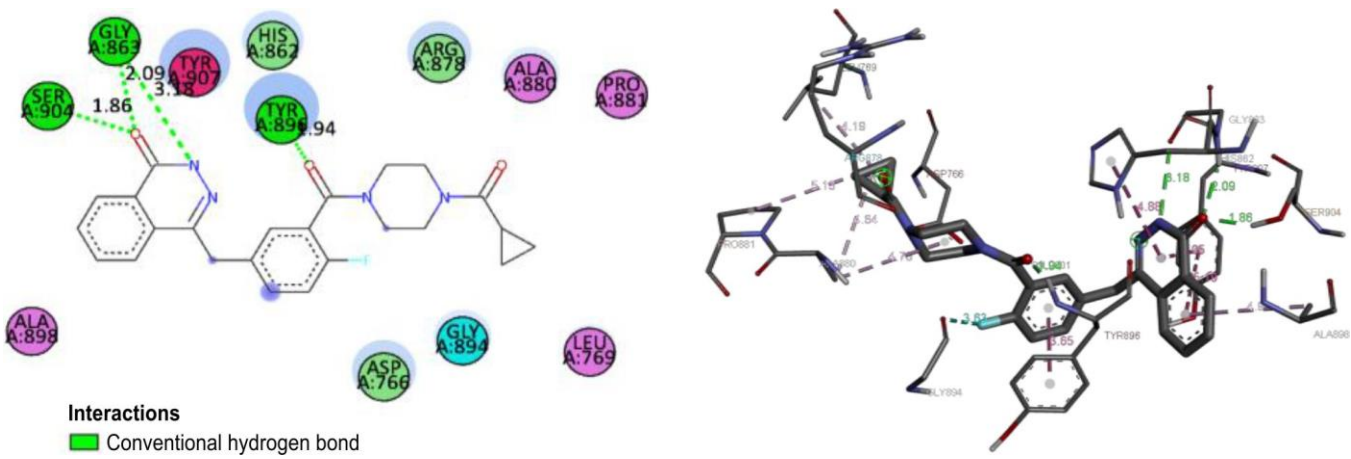

Fig. 1. 2D & 3D interactions of reference molecule with the PARP1 target protein with PDB ID: 7KK4

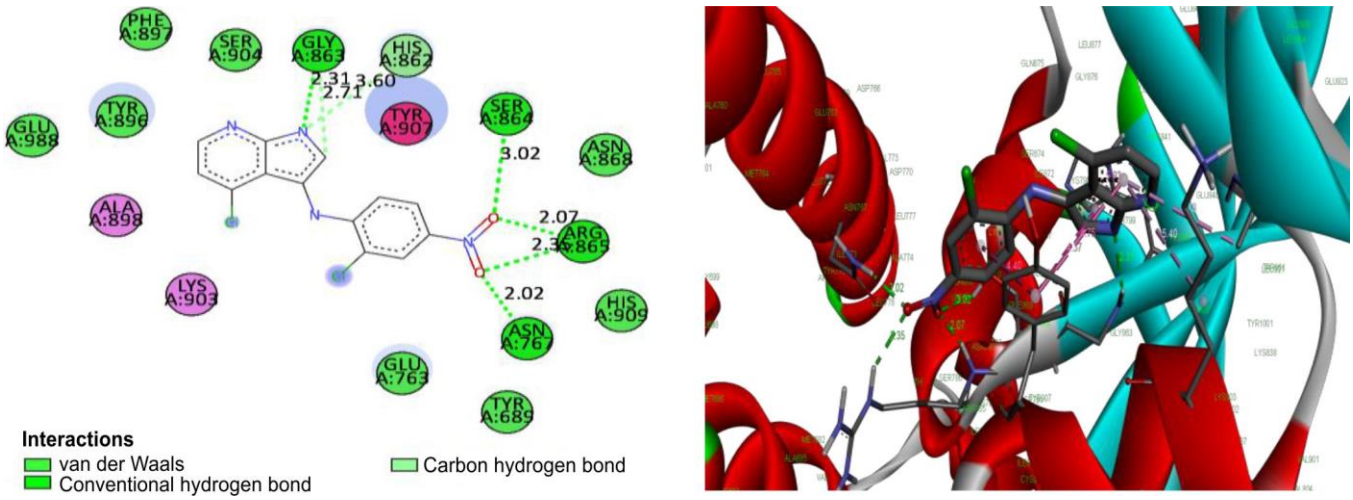

Fig. 2. 2D & 3D interactions of **5e** with the PARP1 target protein with PDB ID: 7KK4

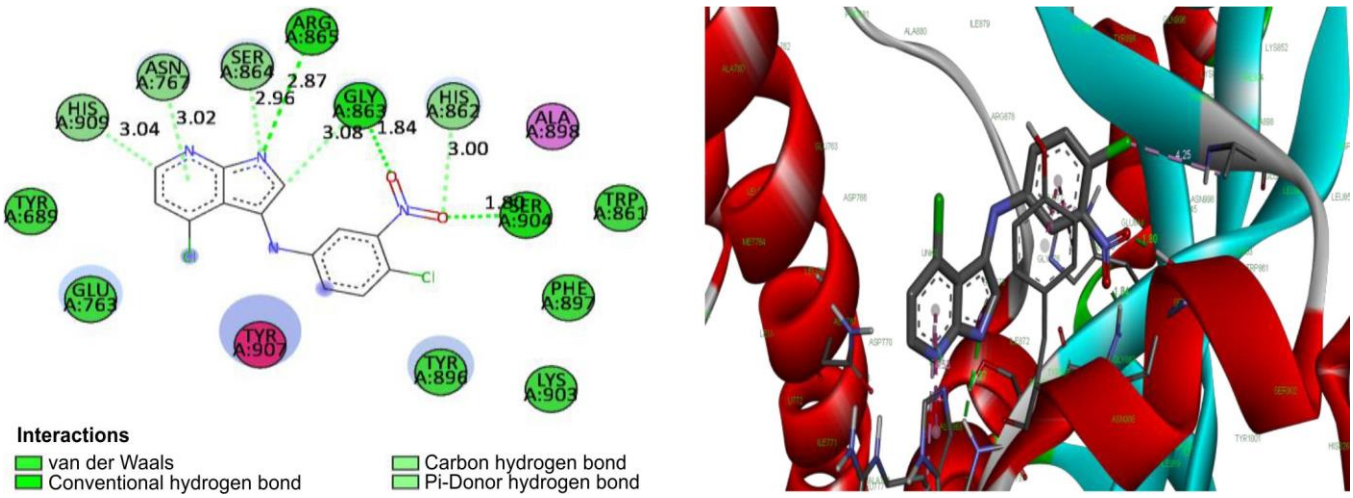

Fig. 3. 2D & 3D interactions of **5c** with the PARP1 target protein with PDB ID: 7KK4

TABLE-2
ANTIPROLIFERATIVE ACTIVITY DATA
OF THE TESTED COMPOUNDS (**5a-h**)

Compd.	GI_{50} (μM)	Compd.	GI_{50} (μM)	Compd.	GI_{50} (μM)
5a	22.14	**5d**	26.41	**5g**	14.21
5b	12.11	**5e**	53.22	**5h**	135.12
5c	122.34	**5f**	15.62	Std.	35.12

may adversely influence receptor interaction and cellular permeability. The biological evaluation suggests that halogen substituted pyrrolo[2,3-*b*]pyridine derivatives possess promising anticancer potential against breast cancer cells, with compound **5b** emerging as the most active analogue of the series.

Conclusion

A novel series of 4-chloro-1*H*-pyrrolo[2,3-*b*]pyridine-3-amine derivatives (**5a-h**) was successfully synthesised from 4-chloro-7-azaindole through a multistep synthetic strategy involving chlorination, cyclisation and nucleophilic substitution reactions. The structures of the synthesised compounds were satisfactorily established using spectral and analytical techniques including ^{1}H NMR, ^{13}C NMR and HRMS analysis. The biological evaluation against MCF-7 human breast cancer cell lines demonstrated that several derivatives possess significant antiproliferative activity. Among the series, compounds **5b**, **5g** and **5f** exhibited the most promising cytotoxic effects with GI_{50} values of 12.11, 14.21 and 15.62 μM, respectively, indicating the favourable influence of halogen-substituted phenyl moieties on anticancer activity. It is observed that the electron-withdrawing substituents enhance the interaction potential and biological performance of the pyrrolopyridine scaffold. Molecular docking studies against the PARP1 receptor protein (PDB ID: 7KK4) further supported the experimental findings by revealing stable ligand–protein interactions within the active binding pocket. Compounds **5e** and **5c** displayed the most favourable binding affinities, attributed to hydrogen bonding, hydrophobic interactions and effective accommodation within the catalytic domain of PARP1.

ACKNOWLEDGEMENTS

The authors are grateful to the Management of Ratnam Institute of Pharmacy, Pidathapolur, Nellore, India, for providing the critical support in completing the current work.

CONFLICT OF INTEREST

The authors declare that there is no conflict of interests regarding the publication of this article.

DECLARATION OF AI-ASSISTED TECHNOLOGIES

During the preparation of this manuscript, the authors used an AI-assisted tool(s) to improve the language. The authors reviewed and edited the content and take full responsibility for the published work.

REFERENCES

1. J. Merour and B. Joseph, *Curr. Org. Chem.*, **5**, 471 (2001); https://doi.org/10.2174/1385272013375427.
2. J.Y. Mérour, F. Buron, K. Plé, P. Bonnet and S. Routier, *Molecules*, **19**, 19935 (2014); https://doi.org/10.3390/molecules191219935
3. Y. Kotaiah, N. Harikrishna, K. Nagaraju and C. Venkata Rao, *Eur. J. Med. Chem.*, **58**, 340 (2012); https://doi.org/10.1016/j.ejmech.2012.10.007
4. R. Tyagi, K. Yadav, N. Srivastava and R. Sagar, *Curr. Pharm. Design*, 30, 255 (2024); https://doi.org/10.2174/0113816128280082231205071504.
5. P.G. Jain and B.D. Patel, *Eur. J. Med. Chem.*, **165**, 198 (2019); https://doi.org/10.1016/j.ejmech.2019.01.024
6. R. Cincinelli, L. Musso, L. Merlini, G. Giannini, L. Vesci, F.M. Milazzo, N. Carenini, P. Perego, S. Penco, R. Artali, F. Zunino, C. Pisano and S. Dallavalle, *Bioorg. Med. Chem.*, **22**, 1089 (2014); https://doi.org/10.1016/j.bmc.2013.12.031
7. C. Marminon, A. Pierré, B. Pfeiffer, V. Pérez, S. Léonce, A. Joubert, C. Bailly, P. Renard, J. Hickman and M. Prudhomme, *J. Med. Chem.*, **46**, 609 (2003); https://doi.org/10.1021/jm0210055
8. M.A. El-Zahabi, R. Yousef, I. Eissa and A. Elwan, *Al-Azhar J. Pharm. Sci.*, **68**, 64 (2023); https://doi.org/10.21608/ajps.2023.332167
9. H. Behbehani, F.A. Aryan, K.M. Dawood and H.M. Ibrahim, *Sci. Rep.*, **10**, 21691 (2020); https://doi.org/10.1038/s41598-020-78590-x
10. A.S. Borude, S.R. Deshmukh, S.V. Tiwari, S.H. Kumar and S.R. Thopate, *Eur. J. Med. Chem.*, **276**, 116727 (2024); https://doi.org/10.1016/j.ejmech.2024.116727
11. R. Wang, Y. Chen, B. Yang, S. Yu, X. Zhao, C. Zhang, C. Hao, D. Zhao and M. Cheng, *Bioorg. Chem.*, **94**, 103474 (2020); https://doi.org/10.1016/j.bioorg.2019.103474
12. M. Alrooqi, S. Khan, F.A. Alhumaydhi, S.A. Asiri, M. Alshamrani, M.M. Mashraqi, A. Alzamami, A.M. Alshahrani and A.A. Aldahish, *Anticancer. Agents Med. Chem.*, **22**, 2775 (2022); https://doi.org/10.2174/1871520622666220324102849
13. L. Long, H. Zhang, Z.H. Zhou, L. Duan, D. Fan, R. Wang, S. Xu, D. Qiao and W. Zhu, *Eur. J. Med. Chem.*, **273**, 116470 (2024); https://doi.org/10.1016/j.ejmech.2024.116470
14. B. Morak-Młodawska, E. Martula, M. Jeleń, A. Beberok, Z. Rzepka, S. Musiał, S. Małek, M. Karkoszka-Stanowska and D. Wrześniok, *Molecules*, **30**, 2779 (2025); https://doi.org/10.3390/molecules30132779
15. T.Y. Shen, T.B. Windholz, A. Rosegay, B.E. Witzel, A.N. Wilson, J.D. Willett, W.J. Holtz, R.L. Ellis, A.R. Matzuk, S. Lucas, C.H. Stammer, F.W. Holly, L.H. Sarett, E.A. Risley, G.W. Nuss and C.A. Winter, *J. Am. Chem. Soc.*, **85**, 488 (1963); https://doi.org/10.1021/ja00887a038
16. R. Prudent, É. Vassal-Stermann, C.H. Nguyen, M. Mollaret, J. Viallet, A. Desroches-Castan, A. Martinez, C. Barette, C. Pillet, G. Valdameri, E. Soleilhac, A. Di Pietro, J.-J. Feige, M. Billaud, J.-C. Florent and L. Lafanechère, *Br. J. Pharmacol.*, **168**, 673 (2013); https://doi.org/10.1111/j.1476-5381.2012.02230.x.
17. R. Pettipher, T.T. Hansel and R. Armer, *Nat. Rev. Drug Discov.*, **6**, 313 (2007); https://doi.org/10.1038/nrd2266
18. L. Zan, H. Wu, J. Jiang, S. Zhao, Y. Song, G. Teng, H. Li, Y. Jia, M. Zhou, X. Zhang, J. Qi and J. Wang, *Neurochem. Int.*, **58**, 872 (2011); https://doi.org/10.1016/j.neuint.2011.02.014
19. S. Rekulapally, R. Jarapula, K. Gangarapu, S. Manda and J.R. Vaidya, *Med. Chem. Res.*, **24**, 3412 (2015); https://doi.org/10.1007/s00044-015-1390-0
20. J. Guillard, M. Decrop, N. Gallay, C. Espanel, E. Boissier, O. Herault and M.-C. Viaud-Massuard, *Bioorg. Med. Chem. Lett.*, **17**, 1934 (2007); https://doi.org/10.1016/j.bmcl.2007.01.033
21. M. Lefoix, G. Coudert, S. Routier, B. Pfeiffer, D.H. Caignard, J. Hickman, A. Pierré, R.M. Golsteyn, S. Léonce, C. Bossard and J.-Y. Mérour, *Bioorg. Med. Chem.*, **16**, 5303 (2008); https://doi.org/10.1016/j.bmc.2008.02.086
22. D.A. Sandham, C. Adcock, K. Bala, L. Barker, Z. Brown, G. Dubois, D. Budd, B. Cox, R.A. Fairhurst, M. Furegati, C. Leblanc, J. Manini, R. Profit, J. Reilly, R. Stringer, A. Schmidt, K.L. Turner, S.J. Watson, J. Willis, G. Williams and C. Wilson, *Bioorg. Med. Chem. Lett.*, **19**, 4794 (2009); https://doi.org/10.1016/j.bmcl.2009.06.042
23. A. Chen, *Chin. J. Cancer*, **30**, 463 (2011); https://doi.org/10.5732/cjc.011.10111
24. N. Sharma and Anurag, *Mini Rev. Med. Chem.*, **19**, 727 (2019); https://doi.org/10.2174/1389557518666180928154004
25. Y.Q. Wang, P.Y. Wang, Y.T. Wang, G.F. Yang, A. Zhang and Z.H. Miao, *J. Med. Chem.*, **59**, 9575 (2016); https://doi.org/10.1021/acs.jmedchem.6b00055.
26. Z. Zhong, L. Shi, T. Fu, J. Huang and Z. Pan, *J. Med. Chem.*, **65**, 7278 (2022); https://doi.org/10.1021/acs.jmedchem.2c00255
27. K. Ryan, B. Bolaños, M. Smith, P.B. Palde, P.D. Cuenca, T.L. Van Arsdale, S. Niessen, L. Zhang, D. Behenna, M.A. Ornelas, K.T. Tran, S. Kaiser, L. Lum, A. Stewart and K.S. Gajiwala, *J. Biol. Chem.*, **296**, 100251 (2021); https://doi.org/10.1074/jbc.RA120.016573
28. BIOVIA, Dassault Systèmes, Discovery Studio Visualizer, ver. 21.1.0.20298, San Diego, CA, USA: Dassault Systèmes (2021).